J Comput Neurosci (2007) 22:301–312
DOI 10.1007/s10827-006-0014-6

Local cortical circuit model inferred from power-law distributed neuronal avalanches

Jun-nosuke Teramae · Tomoki Fukai

Received: 7 April 2006 / Revised: 23 November 2006 / Accepted: 5 December 2006 / Published online: 17 January 2007

Abstract How cortical neurons process information crucially depends on how their local circuits are organized. Spontaneous synchronous neuronal activity propagating through neocortical slices displays highly diverse, yet repeatable, activity patterns called "neuronal avalanches". They obey power-law distributions of the event sizes and lifetimes, presumably reflecting the structure of local circuits developed in slice cultures. However, the explicit network structure underlying the power-law statistics remains unclear. Here, we present a neuronal network model of pyramidal and inhibitory neurons that enables stable propagation of avalanche-like spiking activity. We demonstrate a neuronal wiring rule that governs the formation of mutually overlapping cell assemblies during the development of this network. The resultant network comprises a mixture of feedforward chains and recurrent circuits, in which neuronal avalanches are stable if the former structure is predominant. Interestingly, the recurrent synaptic connections formed by this wiring rule limit the number of cell assemblies embeddable in a neuron pool of given size. We investigate how the resultant power laws depend on the details of the cell-assembly formation as well as on the inhibitory feedback. Our model suggests that local cortical circuits may have a more complex topological design than has previously been thought.

Competing financial interests: The authors declare that they have no competing financial interests.

Action Editor: Peter Latham

J. Teramae · T. Fukai (✉)
Laboratory for Neural Circuit Theory,
RIKEN Brain Science Institute,
Hirosawa 2-1, Wako, Saitama 351-0198, Japan
e-mail: tfukai@brain.riken.jp

J. Teramae
e-mail: teramae@brain.riken.jp

Keywords Neuronal wiring · Synchronization · Cell assembly · Synfire chain · Cortical network development

Cortical microcircuit is the fundamental functional unit of information processing in the cortex, and much effort has been made to clarify the neuronal wiring of cortical neurons (Braitenberg and Schuz, 1998; Holmgren et al., 2003; Gupta et al., 2000; Stepanyants et al., 2004; Kalisman et al., 2005; Foldy et al., 2005; Yoshimura et al., 2005). These studies have revealed many interesting features of the connectivity among a relatively small number of cortical neurons. However, anatomical or electrophysiological methods alone are not powerful enough for revealing the topology of neuronal wiring among thousands, or tens of thousands, of cortical neurons. Another approach is necessary. Here, we attempt to derive a plausible wiring pattern of cortical neurons by asking, theoretically, what explicit network structure may underlie "neuronal avalanches" and their characteristic power-law statistics.

Neuronal avalanches represent temporally precise, spontaneous synchronous activity, and have been recorded in slice cultures of rat layer 2/3 cortex by multi-electrode arrays (Beggs and Plenz, 2003, 2004; Stewart et al., 2004; Vogels et al., 2005). They have significantly varied sizes and lifetimes that are power-law distributed with an exponent of $-3/2$ or -2, respectively. Since a nonlinear dynamical system often exhibits power law statistics when in a certain critical state, Beggs and Plenz (2003) has suggested that neuronal avalanches may represent a critical branching process (Fig. 1(b), *left*) (Harris, 1989; Zapperi et al., 1995).

There are two main schemes for achieving neuronal avalanches. The first is what we call a "critical branching process in activity (CBPA)". In short, the CBPA is an attempt to implement the critical branching process by neuronal populations. In this scheme, an avalanche consists of

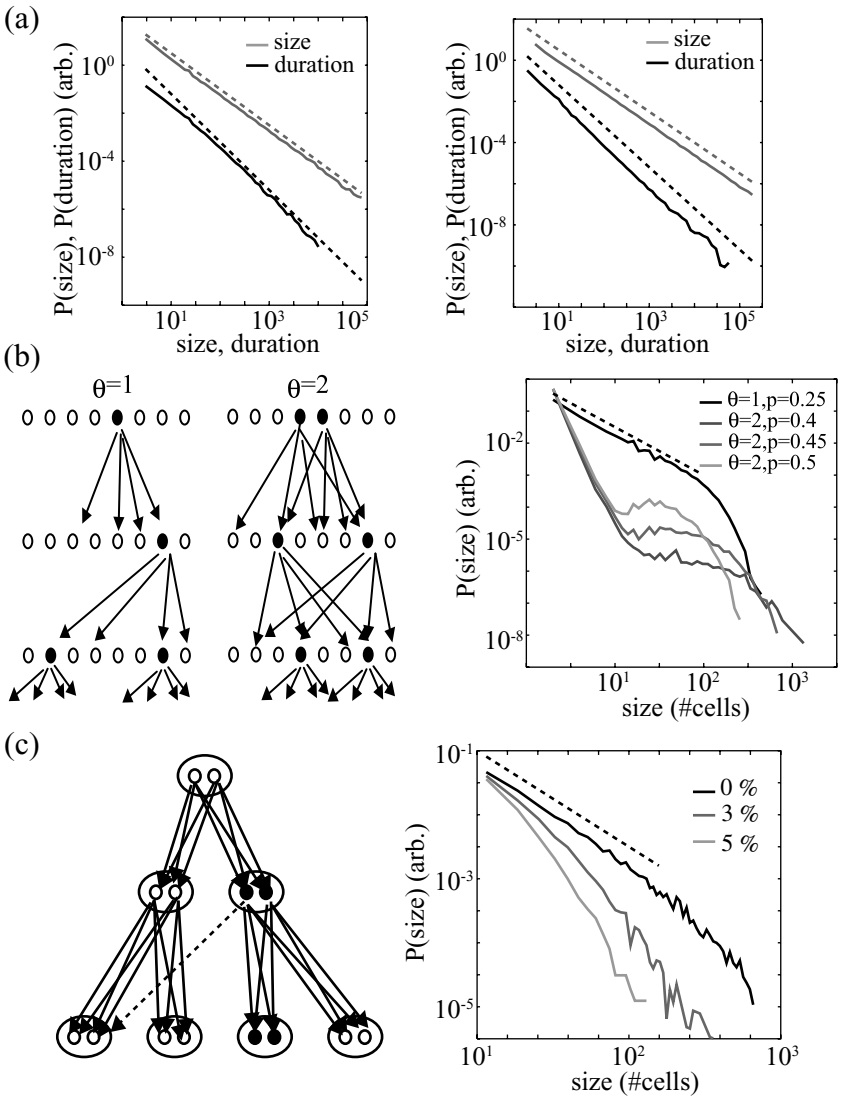

Fig. 1 Breakdown of power laws in CBPA. (a) *Left*, Power-law distributions of event size (*upper trace*) and lifetime (*lower trace*) were calculated for the critical branching process by solving the stochastic Eq. (1a). *Right*, Similar distributions were calculated for the gamma distribution-based wiring process by solving Eq. (2). (b) Branching process models in which each ascendant projecting to four descendants (i.e., branching index $Q = 4$). Activity of each node can propagate to its descendant with probability p, and θ active ascendants are necessary for activating a descendant: $\theta = 1$ and $p = 0.25$ (*solid curve*); $\theta = 2$, $p = 0.4$, 0.45 and 0.5 (*gray curves, from heavy to light*). The dashed line represents an exponent of $-3/2$. (c) Each node is represented by four independent sub-nodes. Each sub-node in an ascendant node projects to all eight sub-nodes in two descendant nodes and activates each descendant sub-node with a probability of 0.955, which is slightly smaller than the critical value $(1/2)^{1/16}$ in the present case. Thus constructed projections were rewired randomly between different nodes in the same generation with a probability of 0 (*solid*), 3 (*gray*) and 5 % (*light gray*). The dashed line represents an exponent of $-3/2$

sequentially activated nodes, where each node is a group of neurons (Fig. 1(c)). Each node projects to Q other nodes, and at criticality, the probability that a node can activate one of its descendant nodes is $1/Q$. Here, a node is active if a large enough fraction of neurons for activating its descendants is active. Importantly, nodes cannot be overlapping, so if a neuron is in one node it is not in any other.

The second scheme is what we call a critical wiring process (CWP). In this scheme, each node projects to exactly one node, and if a node is active, its descendant node is active with probability 1. In addition, nodes can overlap, so a single neuron can belong to more than one node (Fig. 2(a), *right*).

We show in this study that CBPA can exhibit avalanches only if it is finely tuned. Allowing, for example, only a few percent of the neurons to project outside their target nodes destroys power low behavior. This seems inconsistent with known cortical anatomy. The CWP, on the other hand, is highly robust to perturbations. Thus, it represents a much more likely wiring diagram than the CBPA.

To achieve the CWP, we propose a stochastic wiring rule to develop synaptic connections in a population of pyramidal neurons and interneurons. With a simple probability rule to determine the sizes of successive nodes, the wiring process mathematically resembles the branching process. The resultant neuronal wiring is a heterogeneous ensemble of subnetworks that stably propagate avalanche-like synchronous activity consistent with power laws. The topological pattern of this neuronal wiring has not been known previously.

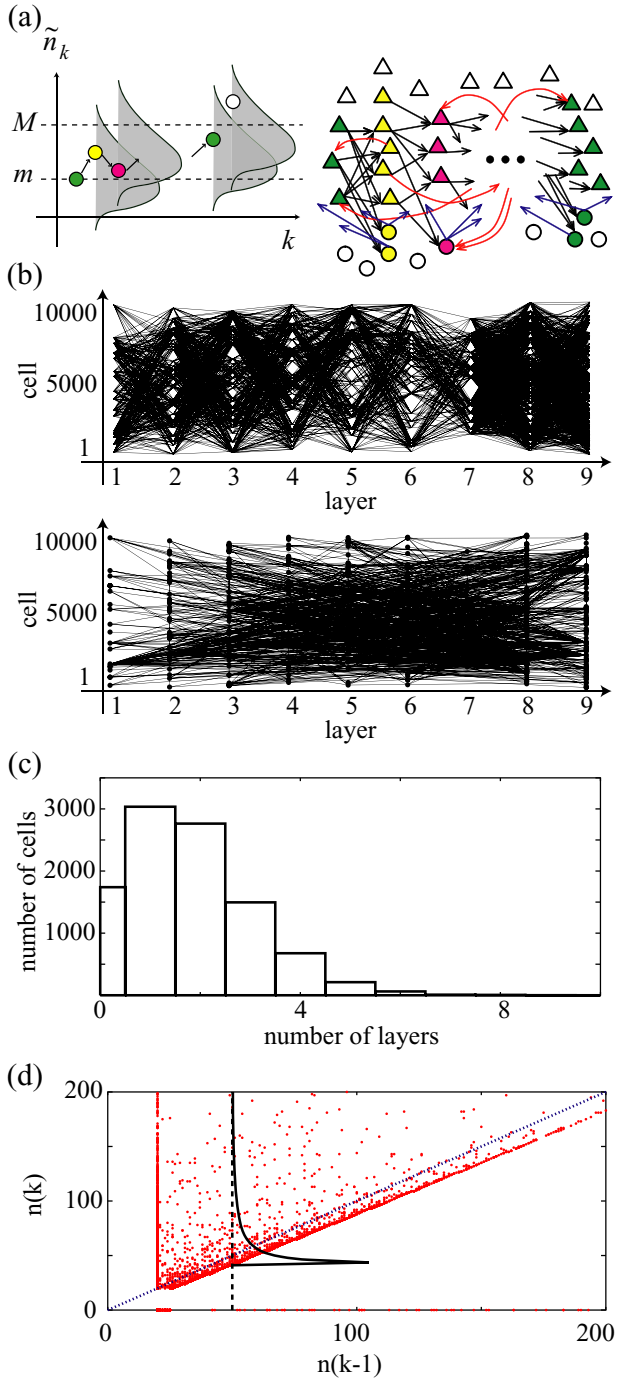

Fig. 2

We may regard the developed network as an ensemble of predominantly feedforward subnetworks ("synfire chains") comprising overlapping cell assemblies. Synfire chains accounted for precisely-timed spike sequences observed in *in vivo* and *in vitro* cortical networks (Abeles, 1991; Prut et al., 1998; Reyes, 2003; Ikegaya et al., 2004; Kitano and Fukai, 2004), and were recently revived as a candidate of the avian neuronal circuits engaging in song learning (Hahnloser et al., 2002; Kimpo et al., 2003). While a purely-feedforward synfire chain has extensively been studied in computational models (Diesmann et al., 1999; Cateau and Fukai, 2001), its generalization with a more realistic wiring pattern of cortical neurons seems difficult (Mehring et al., 2003; Vogels et al., 2005). This study proposes such a generalization in a way that is consistent with neuronal avalanches.

Methods

Wiring procedure

Consider a large pool of N excitatory and $N/4$ inhibitory neurons which initially have no synaptic connections between any neuron pair. Throughout this study, N is set to 10,000. We arrange excitatory and inhibitory neurons into successive cell layers, or nodes, according to the following procedure. We note that layers in this model do not necessarily correspond to cortical layers but they are a metaphor that makes the connectivity or the topology of local cortical circuits

◀ **Fig. 2** The developmental rule and the structure of entangled synfire chains in CWP. Unless otherwise stated, the results are shown for $m = 20$, $\sigma = 4$ and $M = 200$ throughout the paper. (a) The rule for grouping and wiring neurons is schematically illustrated (see Methods for details). First, the sizes of consecutive cell assemblies are determined by a Markov process (*left*), and then the corresponding number of neurons is selected randomly for each cell assembly from an excitatory neuron pool (*right*). Excitatory neurons (*triangles*) in the consecutive layers are connected in a feedforward manner. Each inhibitory neuron (*circle*) receives input from a specific layer, and projects to the excitatory neurons randomly chosen from the entire neuron pool. (b) A 9-layer synfire chain is exemplified in a 10,000-neuron network. *Upper*, Solid lines represent the feedforward connections between consecutive cell assemblies. *Lower*, The same synfire chain automatically involves a considerable number of feedback connections as well as feedforward connections between distant assemblies. These connections represent feedforward connections between adjacent assemblies in other synfire chains, and typically constitute about 10% of all connections in a chain. (c) The number of the cell assemblies to which a neuron belongs obeys a Poisson distribution. (d) The sizes of successive layer pairs ($n(k-1)$, $n(k)$) are plotted with red dots. The conditioned gamma distribution (*bold solid curve*), from which $n(k)$ was sampled, is drawn, being laid down, at $n(k-1) = 50$ for $\alpha = 0.1$ (see also Fig. 5(a) about the profiles of the gamma distributions for different α values). The blue dotted line designates the relationship, $n(k) = n(k-1)$, which is essential for achieving a critical process in the present neuronal wiring (see Eqs. (1) and (2))

easy to visualize. We choose m ($\ll N$) excitatory neurons randomly from the neuron pool and set them to an initial layer of a first chain. Successive layers are constructed by selecting a variable number of excitatory and inhibitory neurons randomly from the neuron pool. Let n_k be the number of excitatory neurons in the k-th layer. Then, n_k is determined according to a stochastic process with a certain conditional probability distribution $P(n_k|n_{k-1})$ that has an average equal to the size n_{k-1} of the preceding layer (Fig. 2(a), *left*). The selection of the number of cells in each layer, being dependent on the previous layer, is a Markov-chain. The selection process is repeated to make consecutive layers in a synfire chain. Each neuron in a layer receives synaptic inputs from m excitatory neurons in the preceding layer. The multiple sets of presynaptic neurons are chosen independently for the individual postsynaptic neurons without any bias (Fig. 2(b), *upper*). As shown later, each layer of excitatory neurons fires synchronously and may define a functional cell assembly in this model.

If the layer size chosen exceeds a certain range at some k, that is, $n_k < m$ or $n_k > M$ ($m < M \ll N$), then the chain is terminated at the $(k-1)$-th layer, and a new chain is started with a new initial layer of m excitatory neurons. The above procedure is repeated to construct sufficiently many chains. The lower bound m is necessary since postsynaptic firing requires a sufficient number of presynaptic spikes. The upper bound M keeps synaptic connections sufficiently sparse (Rolls and Treves, 1998; Brunel, 2000) in order to embed a large number of chains in a given neuron pool. Unless otherwise mentioned, $m = 20$ and $M = 200$.

Inhibitory neurons are introduced in each cell assembly, keeping the number ratio between excitatory and inhibitory neurons at 4:1 (Fig. 2(a), *right*). Thus, layer k contains $n_k/4$ inhibitory neurons. Each inhibitory neuron is projected to by m randomly-chosen excitatory neurons in the preceding layer. However, unlike excitatory neurons that project selectively to neurons in the succeeding layer, the inhibitory neurons project non-selectively to 5% of all excitatory neurons in the entire neuron pool (Fig. 2(a), *right*).

In summary, we can express the synaptic connections from excitatory neuron j to excitatory neuron i as

$$g_{ij} = \sum_{\mu=1}^{P} \sum_{k=1}^{l(\mu)-1} \xi_i^{\mu,k+1} \eta_j^{\mu,k},$$

where P is the total number of synfire chains and $l(\mu)$ is the length of the μ-th chain. The N-dimensional vector $\xi^{\mu,k} = \{\xi_i^{\mu,k}\}_{i=1,\cdots,N}$ represents neurons belonging to the k-th layer in the μ-th chain: $\xi_i^{\mu,k} = 1$ if neuron i belongs to the layer and $\xi_i^{\mu,k} = 0$ otherwise. We derive vector $\eta^{\mu,k}$ from $\xi^{\mu,k}$ by randomly choosing m of the "1" components in $\xi^{\mu,k}$ and setting all other components equal to 0. As expressed by the above synaptic matrix, whenever the same pair of pre- and postsynaptic neurons appears, we increment the corresponding synaptic weight by unit strength.

Regarding $P(n_k|n_{k-1})$, we first consider the case where $P(n_k|n_{k-1})|_{n_{k-1}=n}$ is a Gaussian with mean n and variance $\sigma^2 n$. Note that the value of σ determines the degree to which the size of consecutive layers can vary. However, we find that this distribution cannot account for all the known properties of neuronal avalanches. Therefore, we investigate the case where the distribution is given as $P(n_k;\alpha|n_{k-1})|_{n_{k-1}=n} = P_\Gamma(n_k - n + \sigma\sqrt{\alpha n};\alpha,\sigma\sqrt{n/\alpha})$ in terms of the gamma distribution $P_\Gamma(x;\alpha,\beta) = x^{\alpha-1}\exp(-x/\beta)/\beta^\alpha\Gamma(\alpha)$. As in the first case, this distribution has mean n and variance $\sigma^2 n$ at an arbitrary value of parameter α. Unless otherwise stated, $\alpha = 0.1$ and $\sigma = 4.0$. We also study the case where $P(n_k|n_{k-1})|_{n_{k-1}=n}$ is independent of n and is given as a Gaussian with mean m and variance $\sigma^2 m$ that are common to all layers.

Neuron model

The following membrane potential dynamics closely mimic the firing patterns of cortical neurons (Izhikevich, 2004) and were used in the present simulations:

$$\dot{v} = 0.04v^2 + 5v + 140 - u - g_{\mathrm{AMPA}}(v-0) - g_{\mathrm{GABA}}(v+70)$$
$$\dot{u} = a(bv - u)$$

where $(a, b) = (0.02, 0.2)$ and $(0.1, 0.2)$ for excitatory and inhibitory neurons, respectively. If v reaches 30 mV, it is reset to -65 mV and u is increased by 8 in excitatory neurons and by 2 in inhibitory neurons. On each excitatory or inhibitory neuron, the net conductances of AMPA and GABAergic synapses obey equations of the following form:

$$\dot{g} = -\frac{g}{\tau} + g_{XY}\sum\delta(t - t_{\mathrm{spikes}}) + g_{XY,b}\sum\delta(t - t_{\mathrm{random}}),$$

where $\tau = 5$ and 6 ms for AMPA and GABAergic synapses, respectively. The unit amplitudes of the peak conductance rises, g_{XY}, are set as $g_{\mathrm{EE}} = 0.0105$ for an excitatory-to-excitatory, $g_{\mathrm{EI}} = 0.0075$ for an excitatory-to-inhibitory, and $g_{\mathrm{IE}} = 0.03$ for an inhibitory-to-excitatory synapse. If a pre and postsynaptic neuron pair are connected multiple times in constructing the layers of cell assemblies, the corresponding synapse is increased by the unit. Similarly, $g_{XY,b}$ are set as $g_{\mathrm{EE},b} = 0.009$, $g_{\mathrm{EI},b} = 0.011$, $g_{\mathrm{IE},b} = 0.05$, $g_{\mathrm{II,b}} = 0.05$ and the rates of excitatory and inhibitory background spikes are set as 800 and 200 Hz, respectively such that excitatory and inhibitory neurons may exhibit spontaneous firing of about 1 Hz in the absence of g_{XY}.. It is worth while to note that replacing the above neuron model with

a simpler leaky integrate-and-fire neuron does not affect the power laws in the present network model. The above model, however, allows synchronous activity to propagate at a physiologically realistic speed (about 4 ms per layer), whereas integrate-and-fire neurons require the adjustment of the propagation speed by an explicit inclusion of synaptic delays.

Results

Network topology

Since the power laws of neuronal avalanches coincide with those of a critical branching process, our neuronal wiring rule is based on a Markov stochastic process that mimics the mathematical structure of the branching process. The rule governs the development of synaptic connections in a population of excitatory and inhibitory neurons and creates an ensemble of predominantly feedforward subnetworks of cell assemblies having a variety of sizes (Fig. 2(a): see Methods for details). We note that the wiring rule allows the individual neurons to participate in multiple cell assemblies in the same or different chains (Fig. 2(c)). This makes the neuronal network more complicated than a mere collection of independent purely-feedforward subnetworks: a considerable number of feedback or recurrent connections are also formed within and between the individual chains (Fig. 2(b). *lower*). Suppose that two excitatory neurons belong to adjacent layers in some chain, one belonging to the first layer and the other to the second layer. By construction of the chain, this neuron pair acquires a feedforward connection. If the second neuron participates in another chain, then this synaptic connection that was 'feedforward' in the previous chain, now links the two different chains. If the first neuron also appears in a distant layer of the second chain, the same synaptic connection represents a distant feedforward or feedback connection in this chain. Thus, the functional meaning of a synaptic connection can vary depending on which subnetwork is activated.

The average number of synaptic connections that is not categorized as feedforward connections in a single chain is given as $\frac{Pms^3}{N^2}$, where $s = \sum_{k=1}^{l} n_k$ is the size of the chain (see Appendix). Typically, more than 10% of synaptic connections within a chain constitute such non-feedforward connections when $P = 200$, $N = 10^4$ and $s = m = 20$. The same formula represents the average number of synaptic connections between each pair of different chains. Therefore, the degree of the interferences between different chains is increased with the total number of the embedded cell assemblies. As we will see later, the overlaps between synfire chains restrict the number of the chains embeddable into a neuron pool of given size.

The proposed stochastic wiring rule generates strong correlations between the numbers of neurons in adjacent layers. Figure 2(d) displays the sizes of adjacent layer pairs (n_{k-1}, n_k) in the case where the sizes were determined using the gamma distribution $P(n_k; \alpha | n_{k-1})$ (see Methods). The result indicates the relationship $n_k \approx n_{k-1}$, as expected. The asymmetric distribution of the plots is due to the skewed shape of the gamma distribution. As shown later, the size and lifetime distributions of avalanche-like activities in our model enjoy an excellent agreement with those measured in experiments (Beggs and Plenz, 2003) when we employ the gamma distribution shown in Fig. 2(d) in the wiring rule (see also Fig. 5(a)). We remark that the total amplitudes of synchronous activity recorded in consecutive time bins should exhibit correlations similar to those shown in Fig. 2(d), if the proposed network underlies neuronal avalanches.

Power-law statistics of synchronous activity

In previous experiments, neuronal avalanches were induced in cortical slices by bath application of the glutamate-receptor agonist NMDA and a dopamine D1-receptor agonist (Beggs and Plenz, 2003, 2004). Such neuronal activities exhibited diverse, yet precise spatiotemporal activity patterns, indicating that they were initiated from spontaneous firing of divergent, but fixed subsets of neurons. The present neuron model does not have any intrinsic mechanism to activate the cell assemblies spontaneously. Therefore, in this study synchronous neuronal activity was evoked by a brief external input to the initial layers of individual synfire chains. In doing so, we activated all chains repeatedly with equal probability.

The synchronous activity thus evoked in an arbitrary chain could stably travel to the terminal layer along the chain, irrespective of its length (Figs. 3(a) and (c)). A characteristic feature of the present network model is large fluctuations in the amplitude of a propagating spike packet. To show this, we plotted the time course of the avalanche-like spiking activities traveling through a short and a long chain (Figs. 3(b) and (d)). The large amplitude fluctuations in neuronal activity reflect the fluctuations in the layer size along the chains. During each event of synchronous activity propagation, inhibitory neurons tend to be activated more often than excitatory neurons since they participate on average in more assemblies than excitatory neurons (Fig. 3(e)).

We calculated the size and lifetime distributions of synchronous activity patterns in the case that the cell assemblies were embedded by two Gaussian distributions (Methods). We defined the size of each synchronous activity pattern as the total number of neurons activated in the activity propagation. We find that the size distribution exhibits a power law of exponent $-3/2$ in agreement with experimental results, if the mean of the Gaussian distribution is always reset to the

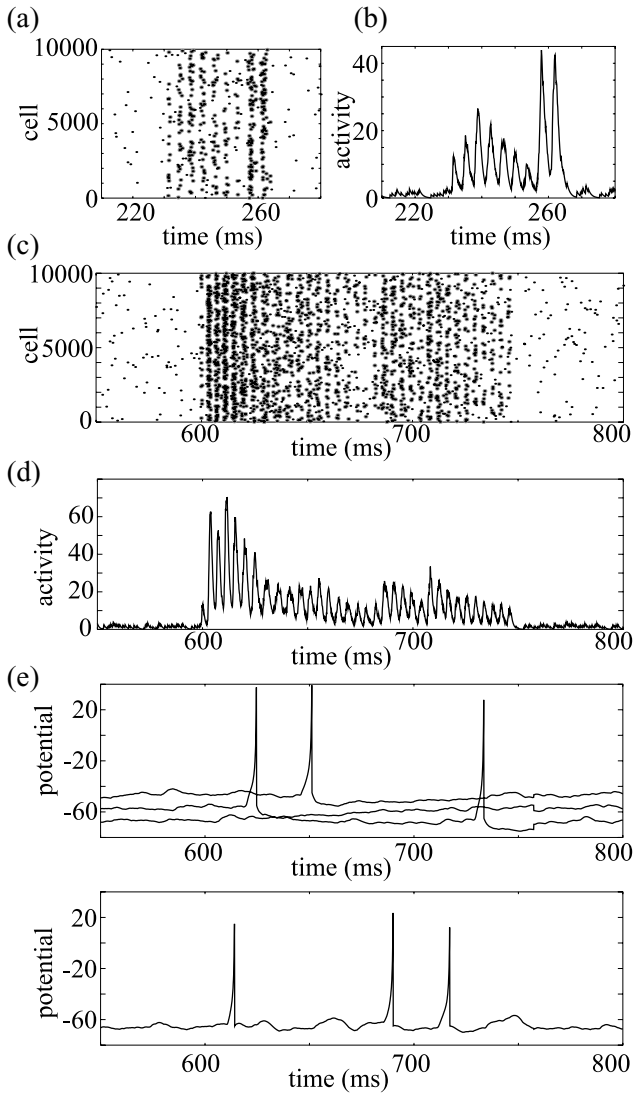

Fig. 3 Synfire neuronal activity showing power-law distributions. In total, 1,000 assemblies were embedded. (a, c) The initial excitatory-cell layer of a relatively short or a relatively long synfire chain was activated by a transient input. The embedded excitatory cell assemblies are shown by gray dots, while the evoked spikes are shown by black dots. (b, d) The neuronal activities propagating through the chains are shown by the sum of excitatory-neuron spikes weighted by exponential factors with a decay constant of 2 ms. The manipulation is almost equivalent to counting the number of spikes in each time bin defined by the time constant. (e) The membrane potentials of three excitatory neurons (*upper*) and an inhibitory neuron (*lower*) during the avalanche-like activity

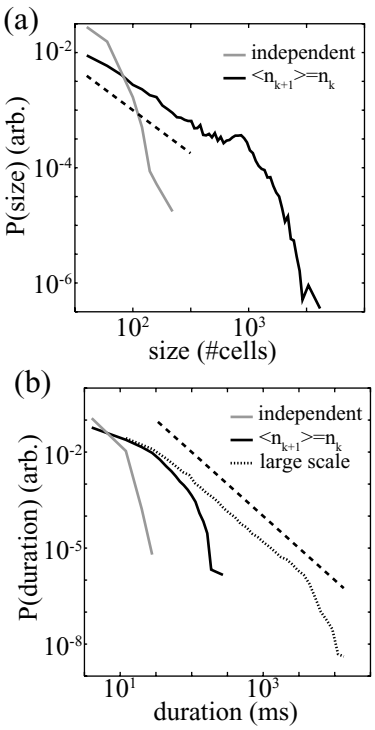

Fig. 4 Power-law distributions of neuronal activity propagating through the synfire chains constructed through the Gaussian-based wiring processes. Parameters were set as $N = 10{,}000$, $M = 200$, $m = 20$, $\sigma = 4$, and 1,000 cell assemblies were embedded. (a) The number of neurons activated in each propagation event is distributed according to a power law of exponent $-3/2$ for a network constructed under the condition $\langle n_{k+1} \rangle = n_k$ (*solid curve*), where n_k is the size of the k-th layer and $\langle \ldots \rangle$ means an expected value. The dashed line designates the desired exponent. If the sizes of the individual layers are independently determined, the distribution shows no power law (*gray curve*). (b) The lifetime distributions obtained with (*solid curve*) and without (*gray curve*) the condition $\langle n_{k+1} \rangle = n_k$. The solid curve deviates from the desired power law of exponent -2 (*dashed line*) in the domain of short lifetimes. A theoretical curve is obtained for a very large-scale network constructed under $\langle n_{k+1} \rangle = n_k$ by solving Eq. (1b) (*gray dotted curve*)

size of the preceding layer during the network construction (Fig. 4(a), *solid curve*). If, however, the mean is fixed at a constant value, the distribution of the avalanche size drops off exponentially without exhibiting a power law (Fig. 4(a), *gray curve*). By contrast, the lifetime distribution deviates from a power law of exponent -2 in both construction methods, especially in the region of short life times (Fig. 4(b), *solid* and *gray curves*). To investigate the deviations more closely, we improved the statistics of sampling the lifetime by solving the discrete-time stochastic equations equivalent to the present wiring process (see Eq. (2) shown later). The results for the lifetime distribution show that the desired exponent can be obtained only in the domain of much longer lifetimes, but not for short ones (Fig. 4(b), *dotted gray curve*: the exponential cut-off is due to the finite-size effect).

In general, power laws are addressed in nonlinear dynamical systems only in the asymptotic domains of physical parameters, which in the present study correspond to large avalanche sizes and long lifetimes. Therefore, the above results may not be surprising. The power law, however, has been revealed in experiments even at rather short lifetimes (< 20–30 ms). It is therefore unlikely that the network models obtained with the Gaussian-based wiring process are consistent with the experimental finding. Below, we show a possible improvement of the present network model.

An improved procedure of neuronal wiring

The Gaussian probability distributions produce both positive and negative fluctuations in the layer size in a symmetric manner. Therefore, the probability that the construction process is terminated within short steps is not so small, implying that the lifetime distribution may be biased towards short lifetimes. To reduce such a bias, we adopted the gamma distribution for embedding the chains of cell assemblies, since the degree of asymmetry with respect to the mean can be modified by changing the value of α (Fig. 5(a)). We found that the resultant distribution of the avalanche size exhibits a power law of exponent $-3/2$ at an arbitrary value of α, as in the previous case (Figs. 5(b) and (d)). By contrast, the distribution of the avalanche lifetime and its exponent in the domain of short lifetimes can significantly vary with the value of α (Fig. 5(c)). We can find such an adequate value of α (≈ 0.1) that sets the exponent equal to -2 (Fig. 5(d): also see Fig. 5(c), *solid curve*). Thus, the behavior of the power-law distribution at short lifetimes can be improved, if the stochastic fluctuations appear asymmetrically in the wiring process.

The value of σ determines the degree to which the size of consecutive layers can vary. This parameter also influences the structure of the embedded synfire chains. If σ is large, the layer size chosen during the stochastic wiring process can easily reach the lower bound. In such a situation, large chains can rarely appear during the wiring process, and neuronal avalanches tend to show an exponential cutoff at relatively small sizes (Fig. 6(a)). On the contrary, if σ is small, the tail of the power law domain extends to rather large avalanche sizes, since such a wiring process can easily generate extremely large-scale synfire chains. This tendency is particularly strong if the gamma distribution is used for neuronal wiring (Fig. 6(b)). However, the process with small σ fails to generate small chains, as understood from the large dips that appear for $\sigma = 4$ and 8 at avalanche sizes smaller than 10^2 (Fig. 6(a)). Therefore, the value of σ needs to be adequately adjusted in order to embed a rich variety of synfire chains into a finite-size neuron pool.

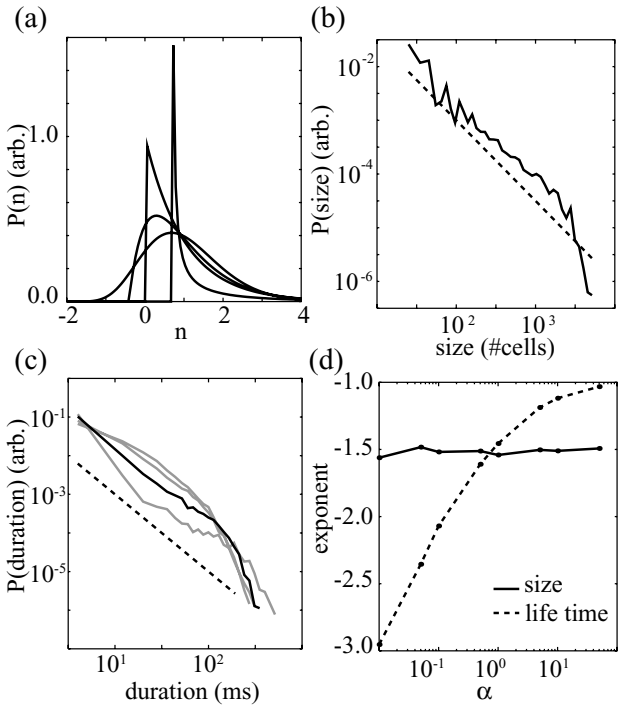

Fig. 5 Power-law distributions of the neuronal activity propagating through the synfire chains constructed using the gamma distributions. Parameters were set as $N = 10{,}000$, $M = 200$, $m = 20$, $\sigma = 4$, and 1,000 chains were embedded. (a) The shape of the gamma distribution changes with the value of parameter α. The distributions were normalized to have a variance of unity, and are shown for $\alpha = 0.01$, 0.1, 1 and 10 in the decreasing order of the peak height. (b) The size of avalanche-like activities is distributed according to a power law of exponent $-3/2$ (*dashed line*) for all the values of α. (c) The lifetime distribution is displayed for the above-mentioned values of α. From the steepest curve, $\alpha = 0.01$, 0.1, 1 and 10. At $\alpha = 0.1$ (*black*), the distribution exhibits a power law of exponent -2 (*dashed line*) even at short lifetimes. (d) The exponents of the size and lifetime distributions are plotted as functions of α

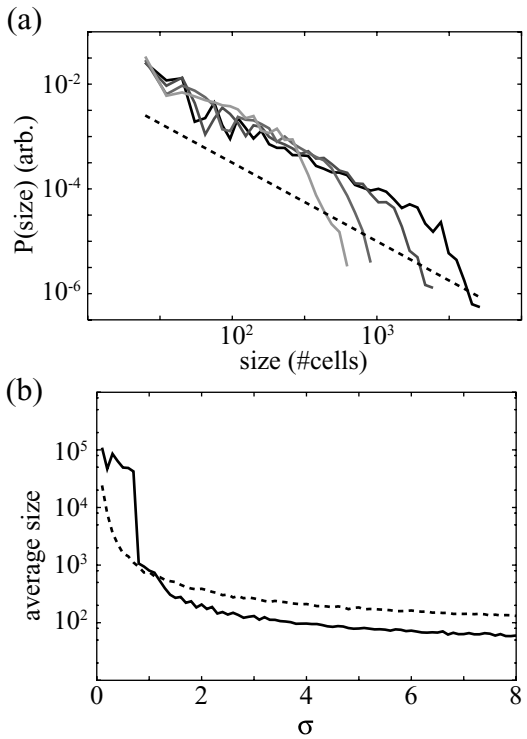

Fig. 6 Effects of the fluctuations in the Markov wiring process on the chain size distributions. (a) From the curves drawn with the lightest gray to black, $\sigma = 4, 8, 16$, and 32. (b) The average chain size is plotted as a function of σ in a network constructed in a population of 10,000 excitatory and 2,500 inhibitory neurons with the gamma (*solid*) or the Gaussian (*dashed*) probability distribution (satisfying $\langle n_{k+1} \rangle = n_k$)

Capacity for embedding cell assemblies

The stability of synchronous activities propagating through the individual chains crucially depends on several factors. Since the synfire chains mutually interact through recurrent synaptic connections, and since the number of such connections is increased with the number of chains, there exists an upper bound for the total number of synfire chains that can be embedded in a given neuron pool. In the present simulations, we were unable to embed more than about 400 chains into a network of 10,000 excitatory and 2,500 inhibitory neurons. If we try to embed more chains, synchronous activity first fails to propagate through relatively long chains, presumably due to a loss of the sparse connectivity (Rolls and Treves, 1998; Brunel, 2000). Therefore, the power law starts to break in the regime of large-scale avalanche-like activity (Fig. 7(a)) in which synchronous activity can easily disperse to multiple synfire chains. The runaway network excitation, however, is eventually terminated by the feedback from inhibitory neurons (Fig. 7(b)). The upper bound for the number of embeddable chains is the cost paid for the multiple recruitments of individual neurons for different cell assemblies. We can avoid unstable activity propagations by constructing mutually non-overlapping cell assemblies. Such an exclusive wiring rule, however, seems unrealistic from a viewpoint of cortical neurobiology (Abeles, 1991). The advantage of the multiple recruitments is that they give an economical representation of cortical cell assemblies, producing more synfire chains with fewer neurons (see Fig. 2(c)).

Inhibition is crucial for stabilizing the avalanche-like synchronous activity, especially if the neuron pool embeds an almost maximal number of synfire chains. To see the role of inhibition in the present network, we reduced the conductance of all GABAergic synapses by about 30% or more. The resultant distributions of the avalanche size show bimodal peaks, and its power-law behaving part exhibits a steeper slope with an exponent smaller than $-3/2$ (Fig. 7(c)). These changes in the profile are consistent with those measured in experiments after the blockade of GABAergic synaptic transmissions by picrotoxin (Beggs and Plenz, 2003). To see how the blockade of inhibition changes the activity propagation, we plotted the time course of coarse-grained spiking activity in Fig. 7(d). Typically, synchronous activity stably propagates through an initial few layers, but it rapidly overflows the synfire chain until an increasing inhibitory feedback abruptly terminates

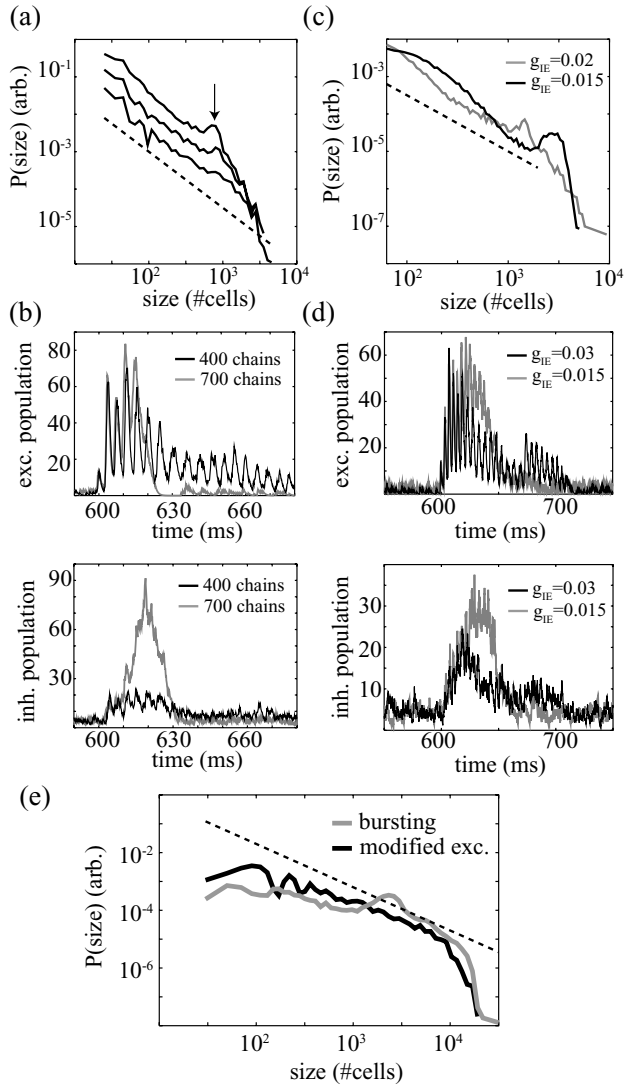

Fig. 7

◀ **Fig. 7** Dynamical properties of the present network model. (a) Capacity for embedding chains of cell assemblies. The avalanche size distribution was calculated in a network with 400, 500 or 700 chains (*curves from below*). The dashed line represents an exponent of $-3/2$. The distributions for 500- and 700-chain networks display notable peaks at a chain size of about 800 cells (*array*), implying that the avalanche-like activity in these networks cannot propagate stably through long chains greater than this size. The results imply that the stability of the avalanche-like activity allows us to embed only about 400 chains into the present neuron pool. (b) The population activities are shown for excitatory (*upper*) and inhibitory (*lower*) neurons during activation of a synfire chain. In total, 400 (*black*) or 700 (*gray*) chains were embedded below or beyond the critical storage capacity, respectively. (c) Reduction of inhibitory synaptic transmissions deteriorates the power-law size distribution: $g_{IE} = 0.02$ (*gray*) and 0.015 (*black*). As inhibitory connections were weakened, the distribution exhibited an exponential-like behavior in the region of avalanche sizes smaller than 10^3 (*black*). In addition, the size distribution developed a hump at relatively large avalanche sizes (*gray* and *black*) since most of large avalanches lost the stability. The dashed line represents an exponent of $-3/2$. (d) The propagating activities of excitatory (*upper*) and inhibitory (*lower*) neurons are shown at a normal ($g_{IE} = 0.03$: *black*) or a reduced ($g_{IE} = 0.015$: *gray*) magnitude of the inhibitory synaptic conductance. (e) The avalanche-size distributions were tested for propagations of spike bursts, with the previous (*gray solid*) or slightly reduced (*black solid*) values of synaptic weights: $g_{EE} = 0.1/20$ and $g_{EI} = 0.07/20$. The dashed line indicates a power of $-3/2$. The neuron model was parameterized as follows: (a, b) = (0.02, 0.2), u was incremented by 2, and the reset potential was -50 mV.

the network activity. Since the runaway activity occurs more often in larger chains, the size distribution exhibits a hump in the domain of large-scale avalanches (Fig. 7(c)).

To see whether the intrinsic properties of neurons may affect the stable activity propagation, we changed the values of model parameters such that the neurons displayed burst of spikes. At a first glance, the changes in the intrinsic properties spoiled the power laws (Fig. 7(e)). However, we could easily recover them by slightly reducing the weights of excitatory synapses. Therefore, the intrinsic properties are not really crucial for the stability of the avalanche–like activities in this model. Our model, with this result, shows an interesting contrast with other mechanisms of neuronal avalanches in which the neuronal dynamics plays an essential role.

Relationship to critical branching process

Why does our network model exhibit the power laws? We can achieve some insight into the mechanism by analyzing the stochastic equation that describes the present process of neuronal wiring and by comparing it with that describing the critical branching process. We note that the number of active nodes at each branching step obeys the following stochastic equations in the critical branching process with Q branches per ascendant (namely, each ascendant node has Q descendant nodes and an active ascendant activates each descendant with a probability of $1/Q$):

$$\langle n_{k+1}\rangle_{n_k=n} = n, \quad \mathrm{var}(n_{k+1})_{n_k=n} = (1-Q^{-1})n, \qquad (k=1,2,\ldots) \tag{1a}$$

where, $\langle\cdots\rangle_{n_k=n}$ represents an average under the condition that the number of excitatory neurons in the preceding layer is n, and the second equation represents the variance. The stochastic variables n_k take only integer values and the initial condition is given as $n_1 = 1$. We can analytically prove that Eq. (1a) displays the power laws with these conditions (Harris, 1989). In the domain where n_k is sufficiently large, the equations can be approximated as

$$n_{k+1} = n_k + \sqrt{(1-Q^{-1})n_k}\,\xi_k. \qquad (k=1,2,\ldots) \tag{1b}$$

Here, $\{\xi_k\}$ $(k = 1, 2,\ldots)$ represents a set of independent normalized Gaussian noise with mean zero, and the process is terminated if n_k reaches zero or exceeds a sufficiently large cut-off value. The size of a branching event is defined as the summation $\sum_k n_k$ taken over all steps preceding the termination of the event.

Similarly, the present wiring process (CWP) can be described as the following Markov stochastic process with respect to $\tilde{n}_k$ ($\equiv n_k/m$), the normalized size of the k-th layer of a synfire chain:

$$\tilde{n}_{k+1} = \tilde{n}_k + \sigma\sqrt{\tilde{n}_k/m}\,X_k. \qquad (k=1,2,\ldots) \tag{2}$$

Here, the initial condition is given as $\tilde{n}_1 = 1$. The noise $\{X_k\}$ is taken to be the Gaussian or the gamma distribution used in constructing synfire chains, with the variance normalized to be unity. Thus, we find that the two processes are governed by quite similar stochastic evolutionary rule. In fact, we can show by numerically solving Eqs. (1b) and (2) that both stochastic processes display power laws of exponent -3/2 and -2 in the distributions of the event size and lifetime (Fig. 1(a)). However, the figure shows that only the process (2) with a particular gamma distribution ($\alpha = 0.1$) can produce the desired power law in the domain of short lifetimes.

In addition to the deviations at short lifetimes, CBPA, where activity propagation is implemented by a cortical neuronal network may suffer other difficulties. Below, we present two typical examples. In Fig. 1(b), we modified the original critical branching process such that activation of a descendant required activation of more than one ascendant. This should be the case if each node in the signaling cascade corresponds to a single neuron. We find that the size distribution shows no power law in such cases. Next, we represented each node of the signaling cascade with multiple neuron-like subunits (Fig. 1(c)). Each ascendant node projected to two descendant nodes and, as in the critical branching process, a single ascendant node could activate a descendant node. The probability of activation was adjusted such that an active ascendant activated only one descendant node on average (see the figure legend). As far as the projections to different descendant nodes are highly selective, the size distribution exhibits the desired power law. If, however, small fractions of the projections are intermingled, the power law easily disappears. Thus, CBPA implemented by the signaling cascade of neuron-like elements is structurally unstable.

Discussion

The power-law statistics of spontaneous synchronous cortical activity have led us to formulate the CWP, a neuronal wiring rule that develops synaptic connections in a large population of excitatory and inhibitory neurons. The CWP determines the topological structure of the local cortical circuit model. We have demonstrated that the CWP is essential for the power-law statistics of synchronous activity propagating through the developed feedforward networks. We have revealed that the exponent of the power-law lifetime distribution is sensitive to the statistical rule governing the neuronal wiring, whereas the exponent of the size distribution is much more robust. The number of synfire chains

embeddable into a given neuron pool is limited by the stability of the avalanche-like activity, and inhibitory neurons significantly enhance this stability.

Critical process in activity propagation vs. neuronal wiring

The activity propagation obeying the critical branching process (CBPA) was suggested as a mechanism of neuronal avalanches (Beggs and Plenz, 2003), and a simple growth model to develop such an activity propagation was recently proposed (Abbott and Rohrkemper, 2006). In fact, a power law of exponent $-3/2$ was analytically derived in the avalanche dynamics of a globally coupled system of non-leaky integrate-and-fire units (Eurich et al., 2002; Levina et al., 2006). However, a similar system of leaky integrate-and-fire neurons exhibits the power law only if the leak time constant is much longer than the typical time scale of activity propagation (Corral et al., 1995). Moreover, we have proven it difficult to formulate the avalanche dynamics with neuron-like processing units. To obtain the power laws, cell assemblies should have no mutual overlaps (Fig. 1). However, such an exclusive subnetwork organization seems to be unrealistic. We note that here the causes of the difficulty are not only fine-tuning of synaptic weights, but also the formation of highly exclusive cell assemblies. Therefore, learning rule may not resolve the difficulty in the scenario that neuronal avalanches emerge from the critical neuronal dynamics.

By contrast, we propose that a critical process should govern the developmental process of neuronal wiring among cortical neurons (CWP), and that the mathematical procedure underlying this process should be similar to that of the branching process. According to this view, neuronal avalanches and their power-law distributions reflect the predominantly feedforward structure and the same statistical distributions of thus developed local cortical networks, respectively. The core of the stochastic wiring process is that it attempts to equate the size of a succeeding layer to that of the current layer (i.e., $\langle n_{k+1} \rangle = n_k$) in constructing each synfire chain (Fig. 4). We have analyzed how the power laws are affected by the details of this stochastic wiring rule (Fig. 5).

The essential novelty of our results is that they explain the mechanism of neuronal avalanches without relying on the neuronal dynamics. Actually, we have shown that the stability and power-law statistics of the avalanche-like activities depend solely on the special topology of neuronal wiring, but not much on the neuronal dynamics (Fig. 7(e)). In fact, neuronal avalanches were observed in acute slices obtained from the rat brain of 4-8 postnatal weeks (Beggs and Plenz, 2003), which were just within the peak critical period of the development of cortical circuits (Mataga et al., 2004; Hensch and Stryker, 2004). Our results suggest that neuronal wiring with the proposed topology should be developed in cortical slice cultures during the critical period.

Lifetime vs. size distributions of avalanche-like neuronal activities

We have tested the power-law distributions of the avalanche size and lifetime in neuronal networks constructed with various probability distributions of the consecutive layer sizes. The distribution of the avalanche size exhibits a power of $-3/2$, if the mean of such a probability distribution coincides with the size of the preceding layer during the construction process (Figs. 4(a) and 5(b)). The exponent appears to be quite universal across different probability distributions. Similarly, the lifetime distribution generally displays a power law of exponent -2 in the asymptotic region of long lifetimes ($>$ several seconds). At short lifetimes, however, the distribution in general shows non-negligible deviations from the power law (Fig. 4(b)). Our model has shown that the gamma distribution-based wiring process with an adequate value of α (≈ 0.1) can replicate the desirable exponent of the lifetime distribution (Figs. 5(c) and (d)). In contrast, it seems difficult to account for the experimental observation by the Gaussian-based neuronal wiring processes. Thus, the lifetime distributions of neuronal avalanches may carry rich information about the local cortical circuit structure.

Capacity of embedded chains and roles of interneurons

The neuronal wiring proposed here generates predominantly feedforward, multiply overlapping chains of cell assemblies (Abeles, 1991) in a manner consistent with recent experimental findings. A considerable number of recurrent synaptic connections are also created, which may destroy the stability of synchronous neuronal activity (Aviel et al., 2005). In fact, a neuron pool of given size can accommodate only a limited number of synfire chains, since embedding more chains creates more recurrent synaptic connections within and between them. In fact, the entangled synfire chains constructed with $N = 10{,}000$ and $M = 200$ can store about 1,000 cell assemblies, or about 400 synfire chains. If this upper bound is not obeyed, synchronous neuronal activity cannot propagate stably through a chain, especially a long one (Figs. 7(a)–(c)). Thus, the present neuronal network somewhat resembles the associative memory model of binary neurons, in which the crosstalk between memorized, stationary or temporal, activity patterns severely limits the storage capacity (Hopfield, 1982; Amit et al., 1985; Amari, 1988; Sompolinsky and Kanter, 1986; Shiino and Fukai, 1993).

Our model demonstrates that inhibitory interneurons play a crucial role in improving the stability of synchronous activity propagating through a long chain (Aviel et al., 2005; Moradi, 2004). The reduction of inhibitory synapses results

in runaway network excitation in our model, and produces a hump in the distribution of the avalanche size (Fig. 7(c) and (d)). Such a hump was actually observed in experiments when $GABA_A$ receptor antagonist picrotoxin was applied to neocortical slices (Beggs and Plenz, 2003). In addition, the enhanced stability greatly contributes to the storage ability of the proposed network model: our prototype model with 10,000 excitatory neurons and no inhibitory neurons could embed at most 200 chains, which correspond to about the half of the present storage capacity (Teramae and Fukai, 2005). Interneurons might also provide a mechanism to limit the size of a synchronously activated cell assembly (i.e., the value of M). This possibility, however, is open for further investigations.

Implications in cortical neurobiology

It has been shown that layer 2/3 cortical neurons form relatively independent, fine-scale subnetworks of selectively interconnected neurons (Yoshimura et al., 2005). Adjacent layer 2/3 pyramidal neurons often share common excitatory input within layer 2/3 and from layer 4 when they are connected to each other. By contrast, layer 2/3 neurons share inhibitory input from layers 2/3 and 4 regardless of the synaptic contacts between them. These patterns of neuronal wiring resemble those proposed in this modeling study. It may be the case that multiple entangled synfire chains characterize the network topology of layer 2/3 local cortical circuits.

We note that the power laws in neuronal avalanches do not imply that the underlying network should be scale-free. The number of links at each node exhibits a power-law distribution in a scale-free network (Barabasi and Albert, 1999). However, this does not mean that the synchronous activities propagating through such a network also obeys power laws. In fact, the number of synaptic connections obeys a Poisson distribution in this model (Fig. 2(c)), since the small number of neurons belonging to each cell assembly were randomly chosen from a large neuron pool.

A major limitation of our model is that it does not clarify the biological mechanisms to achieve the proposed neuronal wiring in the developing cortical circuits (Peinado, 2000; Khazipov et al., 2004). The feedforward synaptic connections may be self-organized by spike-timing-dependent plasticity (Levy et al., 2001; Kitano et al., 2002; Izhikevich et al., 2004), which strengthens or weakens pyramidal-to-pyramidal synapses in a temporally asymmetric manner (Bi and Poo, 2001). However, the proposed wiring rule requires additional mechanisms to regulate the size of each cell assembly relative to that of the preceding one. This regulation is possibly activity-dependent, as the total activity in a cell assembly increases in proportion to its size. The processes of axon branching and synapse formation are known to be activity-dependent (Alsina et al., 2001; Uesaka et al., 2005), but little is known about how the spatial pattern of neuronal wiring is determined in these processes. Another limitation of our model is that it has no mechanism to generate the avalanche-like activity sequences spontaneously. These points remain open for future studies.

Appendix

The average number of synaptic connections

In the proposed model, the number of excitatory connections included in the entire network is approximately given as Pms under sparseness assumption where we can neglect a small overlap between different chains ($P,\ s \ll N$), where P is the total number of synfire chains, m is the number of synaptic projections to each cell, and s is the average size of these chains. The connection probability is therefore given as $c = \frac{Pms}{N^2}$. For a chain of average size s, the product of the probability c and the number of possible neuron pairs s^2 gives the average number of non-purely feedforward (recurrent) connections in this chain, $\frac{Pms^3}{N^2}$. We note that the ratio of the number of recurrent connections to that of purely feedforward connections in this chain is $\frac{Pms^3}{N^2}/ms = P\left(\frac{s}{N}\right)^2$. We can similarly obtain the same formula for the average number of synaptic connections between each pair of different chains. This implies that the degree of interferences between synfire chains increases with P.

Acknowledgments The authors express their sincere thanks to T. Hensch and N. Yamamoto for fruitful discussions about the development of the cortical circuits. The present work was partially supported by Grants in Aid for Scientific Research of Priority Areas and Grant-in-Aid for Young Scientists (B) from the Japanese Ministry of Education, Culture, Sports, Science and Technology.

References

Abbott LF, Rohrkemper R (2006) A simple growth model constructs critical avalanche networks. Prog. Brain Res. in press.

Abeles M (1991) Corticonics: Neural Circuits of the Cerebral Cortex. Cambridge University Press, Cambridge.

Alsina B, Vu T, Cohen-Cory S (2001) Visualizing synapse formation in arborizing optic axons in vivo: dynamics and modulation by BDNF. Nat. Neurosci. 4: 1093–1101.

Amari S (1988) Associative memory and its statistical neurodynamical analysis. In: Neural and synergetic computers. Haken H (ed.) Springer-Verlag, Berlin, pp. 85–99.

Amit DJ, Gutfreund H, Sompolinsky H (1985) Storing infinite numbers of patterns in a spin-glass model of neural networks. Phys. Rev. Lett. 55: 1530–1533.

Aviel Y, Horn D, Abeles M (2005) Memory capacity of balanced networks. Neural Comp. 17: 691–713.

Barabasi AL, Albert R (1999) Emergence of scaling in random networks. Science 286: 509–512.

Beggs JM, Plenz D (2003) Neuronal avalanches in neocortical circuits. J. Neurosci. 23: 11167–11177.

Beggs JM, Plenz D (2004) Neuronal avalanches are diverse and precise activity patterns that are stable for many hours in cortical slice cultures. J. Neurosci. 24: 5216–5229.

Bi G, Poo M (2001) Synaptic modification by correlated activity: Hebb's postulate revisited. Annu. Rev. Neurosci. 24: 139–166.

Braitenberg V, Schuz A (1998) Cortex: Statics and Geometry of Neuronal Connectivity. Springer-Verlag, Berlin.

Brunel N (2000) Dynamics of sparsely connected networks of excitatory and inhibitory spiking neurons. J. Comput. Neurosci. 8: 183–208.

Cateau H, Fukai T (2001) Fokker-Planck approach to the pulse packet propagation in synfire chain. Neural Netw. 14: 675–685.

Corral A, Perez CJ, Diaz-Guilera A, Arenas A (1995) Self-organized criticality and synchronization in a lattice model of integrate-and-fire oscillators. Phys. Rev. Lett. 74: 118–121.

Diesmann M, Gewaltig M, Aertsen A (1999) Stable propagation of synchronous spiking in cortical neural networks. Nature 402: 529–533.

Eurich CW, Herrmann JM, Ernst UA (2002) Finite-size effects of avalanche dynamics. Phys. Rev. E 66: 066137-1-15

Foldy C, Dyhrfjeld-Johnsen J, Soltesz I (2005) Structure of cortical microcircuit theory. J. Physiol. 562: 47–54.

Gupta A, Wang Y, Markram H (2000) Organizing principles for a diversity of GABAergic interneurons and synapses in the neocortex. Science 287: 273–278.

Hahnloser RH, Kozhevnikov AA, Fee MS (2002) An ultra-sparse code underlies the generation of neural sequences in a songbird. Nature 419: 65–70. Erratum in: Nature (2003) 421: 294.

Harris TE (1989) The Theory of Branching Processes. Dover, New York.

Hensch TK, Stryker MP (2004) Columnar architecture sculpted by GABA circuits in developing cat visual cortex. Science 303: 1678–1681.

Holmgren C, Harkany T, Svennenfors B, Zilberter Y (2003) Pyramidal cell communication within local networks in layer 2/3 of rat neocortex. J. Physiol. 551: 139–153.

Hopfield JJ (1982) Neural networks and physical systems with emergent collective computational abilities. Proc. Natl. Acad. Sci. U.S.A. 79: 2554–2558.

Ikegaya Y, Aaron G, Cossart R, Aronov D, Lampl I, Ferster D, Yuste R (2004) Synfire chains and cortical songs: temporal modules of cortical activity. Science 304: 559–564.

Izhikevich EM (2004) Which model to use for cortical spiking neurons? IEEE Trans. Neural. Netw. 15: 1063–1070.

Izhikevich EM, Gally JA, Edelman GM (2004) Spike-timing dynamics of neuronal groups. Cereb. Cortex 14: 933–944.

Kalisman N, Silberberg G, Markram H (2005) The neocortical microcircuit as a tabula rasa. Proc. Natl. Acad. Sci. U.S.A. 102: 880–885.

Khazipov R, Sirota A, Leinekugel X, Holmes GL, Ben-Ari Y, Buzsaki G (2004) Early motor activity drives spindle bursts in the developing somatosensory cortex. Nature 432: 758–761.

Kimpo RR, Theunissen FE, Doupe AJ (2003) Propagation of correlated activity through multiple stages of a neural circuit. J. Neurosci. 23: 5750–5761.

Kitano K, Cateau H, Fukai T (2002) Self-organization of memory activity through spike-timing-dependent plasticity. Neurorep 13: 795–798.

Kitano K, Fukai T (2004) Temporal characteristics of the predictive synchronous firing modeled by spike-timing-dependent plasticity. Learn. Mem. 11: 267–276.

Levina A, Herrmann JM, Geisel T (2006) Dynamical Synapses give rise to a power-law distribution of neuronal avalanches. Adv. in Neural Information Processing Systems.

Levy N, Horn D, Meilijson I, Ruppin E (2001) Distributed synchrony in a cell assembly of spiking neurons. Neural Netw. 14: 815–824.

Mataga N, Mizuguchi Y, Hensch TK (2004) Experience-dependent pruning of dendritic spines in visual cortex by tissue plasminogen activator. Neuron 44: 1031–1041.

Mehring C, Hehl U, Kubo M, Diesmann M, Aertsen A (2003) Activity dynamics and propagation of synchronous spiking in locally connected random networks. Biol. Cybern. 88: 395–408.

Moradi F (2004) Information coding and oscillatory activity in synfire neural networks with and without inhibitory coupling. Biol. Cybern. 91: 283–294.

Peinado A (2000) Traveling slow waves of neural activity: a novel form of network activity in developing neocortex. J. Neurosci. 20: RC54:1–6.

Prut Y, Vaadia E, Bergman H, Haalman I, Slovin H, Abeles M (1998) Spatiotemporal structure of cortical activity: properties and behavioral relevance. J. Neurophysiol. 79: 2857–2874.

Reyes AD (2003) Synchrony-dependent propagation of firing rate in iteratively constructed networks in vitro. Nat. Neurosci. 6: 593–599.

Rolls ET, Treves A (1998) Neural Networks and Brain Function. Oxford University Press, New York.

Shiino M, Fukai T (1993) Self-consistent signal-to-noise analysis of the statistical behavior of analog neural networks and enhancement of the storage capacity. Phys. Rev. E 48: 867–897.

Sompolinsky H, Kanter I (1986) Temporal association in asymmetric neural networks. Phys. Rev. Lett. 57: 2861–2864.

Stepanyants A, Tams G, Chklovskii DB (2004) Class-specific features of neuronal wiring. Neuron 43: 251–259.

Stewart CV, Gerfen CR, Plenz D (2004) Dopamine facilitates "neuronal avalanches" and "synfire chains" in layer 2/3 of rat somatosensory cortex slices. Abs. Soc. Neurosci.

Teramae J, Fukai T (2005) Neuronal avalanches as a probe for cortical circuit structure. Abs. Soc. Neurosci.

Uesaka N, Hirai S, Maruyama T, Ruthazer ES, Yamamoto N (2005) Activity dependence of cortical axon branch formation: a morphological and electrophysiological study using organotypic slice cultures. J. Neurosci. 25: 1–9.

Vogels TP, Rajan K, Abbott LF.. (2005) Neural network dynamics. Annu. Rev. Neurosci. 28: 357–376.

Yoshimura Y, Dantzker JLM, Callaway EM (2005) Excitatory cortical neurons form fine-scale functional networks. Nature 433: 868–873.

Zapperi S, Baekgaard LK, Stanley HE (1995) Self-organized branching processes: mean-field theory for avalanches. Phys. Rev. Lett. 75: 4071–4074.